Anomalous seismicity preceding the 1999 Izmit event, NW Turkey

Ali.O.Oncel[1] and Tom Wilson[2]
[1]King-Fahd University and [2]West Virginia University

Abstract

The 1999 Izmit earthquake (17/08/1999, M_w=7.4) was one of the largest earthquakes to occur in northwestern Turkey during the past 100 years. This earthquake occurred along the Izmit-Sapanca fault within the Northern Anatolian Fault Zone. Variations in the generalized fractal dimensions (Dq) of clustering in time and space, the Gutenberg-Richter b value, and earthquake frequency (N) are evaluated in detail over an 8 year time period preceding the Izmit event. Spatial and temporal comparisons of the variations in these parameters reveal anomalous intermediate term behavior over shorter time scales than previously observed. Significant correlation is observed between changes in *b*-value with the spatial and temporal fractal dimension of epicenter distribution. These correlations oscillate back and forth over 2 to 3 year time intervals and suggest occurrence of significant instability in the nature of intermediate-term deformation along the fault zone. Seismotectonic behavior immediately preceding the Izmit event is represented by an excessive rise in *b* value to a maximum of 2.26 accompanied by relatively small increases in D. The rapid rise of *b* is associated with an increased frequency of low magnitude seismicity. Although D (spatial and temporal) increase, they remain less than 1 indicating that seismicity remains clustered prior to rupture. In areas where earthquake frequency or station density do not permit resolution of short term variations of *fractal scaling parameters* within a few months of main rupture, an accelerated period of low magnitude seismicity (high b value) concentrated

along a fault zone (D < 1) may suggest heightened probability of a forthcoming large event.

1. Introduction

Precursory anomalies preceding a large magnitude earthquake can be divided into long-term (10-30 years), intermediate (1 month to 10 years) and short-term (hours to weeks) (Scholz, 2002). Precursory variations in the fractal properties of seismicity distribution may serve as an intermediate warning of future mainshocks (e.g., Main, 1996, Henderson et al., 1994; Nakaya and Hashimoto, 2002; Scholz, 2002). Henderson and Main (1992) and Henderson et al., (1992) examine temporal changes in *b* value, D_S (spatial fractal dimension) and the correlation between them prior to rupture in laboratory triaxial stress tests. Their laboratory tests reveal a gradual rise in *b* followed by a gradual fall. Prior to the California Coalinga earthquake in 1983; *b* value rose gradually for more than a year to ~2.25 and then fell abruptly over a 2 to 3 month period to about 1.8 at the time of rupture. Oscillations in *b* value from high to low and back again occurred at 4 and 6 year intervals in the 10 years preceding the Coalinga event. The intermediate term increases in *b* value were followed by a sharp, short-term, decrease prior to the major event. Oscillations in the fractal pattern of seismicity were observed preceding Western Tottori earthquake (M=7.3) (see Figure 4 of Nakaya and Hashimoto, 2002). Cyclical variations included a decrease in fractal dimension preceding a period during which the fractal dimension rose to a maximum at the time of the main shock.

Temporal variations of *b*-value were used by Henderson and Main (1992) to distinguish between positive and negative feedback fault interactions. Negative feedback

processes are associated with widely distributed fault systems. Fault growth in response to applied stress reduces the stress intensity in the vicinity of the fault and further growth of the fault. There is a negative feedback between increased fault length and stress intensity. Sets of widely distributed, non-interacting, faults deform gradually through time. Individual faults do not accelerate to failure because of the negative feedback between fault extension and local stress intensity: fault tip failure and extension automatically reduce stress concentration and further fault propagation. If, on the other hand, the fault density increases to the point where stress intensity at the tip of the fault is influenced by neighboring faults, then a runaway positive feedback process can develop such that stress intensity increases with fault length. Development of a positive feedback response leads to rapid failure.

The negative feedback process is associated with distributed fault systems. Such systems have D_0 (fractal dimension determined from box counting) greater than 1. Fault rupture is generally restricted to faults of relatively small length and surface area so that *b* tends to be relatively large: D_0 and *b* increase together leading to a positive correlation (see Henderson and Main, 1992). Transition to a positive feedback process is defined by clustering of larger magnitude seismicity and also yields a positive correlation between *b* and D_0. As faults begin to coalesce (i.e. become clustered), earthquake magnitude increases with increasing fault length and area: both D_0 and *b* decrease together.

In this study, we focus on the evaluation of relationships between *b* and D_q along the Izmit-Sapanca fault in the 8 years prior to the 1999 Izmit event. The multifractal dimension D_q was evaluated in time and space; q varied from 2 to 15. Analysis of temporal variability in the spatial correlation dimension (D_2) along major subdivisions of

the central and western parts of NAFZ documented in earlier work (Öncel et al., 1995; Oncel et al., 1996; Oncel and Wilson, 2002) revealed significant changes through time in seismic clustering (D_2). Prior analysis of changes in spatial D_2 (fractal dimension of seismicity distribution) along the NAFZ have also been correlated to changes in *b* value (Öncel et al., 1995; Oncel et al., 1996; Oncel and Wilson, 2002). Some of these correlations may be due to changes in station density (*Öncel et al.*, 1995), while others reflect changes of tectonic interaction (*Oncel et al.*, 1996). Recent evaluation of these relationships reveals significant change in the correlation between D and *b* preceding the Izmit event (*Oncel and Wilson*, 2002 and 2004).

The Izmit event is the first Anatolian event for which of the preceding seismicity has been continuously monitored by a single modern seismological network (MARNET). The Izmit earthquake (M_w=7.4) is associated with rupture of the Izmit-Sapanca fault which is the northern strand of the NAFZ extending from Adapazari at about 31^o E through the Marmara Sea to 29^o E (Figure 1). Earthquake distribution (Figure 1) suggests that this fault coincides with a potential seismic gap across the Lake Sapanca area (Toksoz et al., 1979) or asperity (Oncel and Wyss, 2000a; Oncel and Wyss, 2000b). In this paper, we characterize seismicity using multifractal evaluation of seismicity distribution (D_q) in time and space, the Gutenberg-Richter *b* -value and the event rate (N). To our knowledge, this study is the first to evaluate and compare multifractal behavior of precursory seismicity in both time and space. Comparisons of these parameters are made for the time interval extending from January 5, 1991 through June 6, 1999 (ending approximately two months prior to the Izmit event). Changes in these parameters and their interrelationship through time will be used to draw inferences about potential

variations in underlying crustal stress leading to final rupture of the Izmit-Sapanca fault zone.

Maximum strain distribution through the region (Figure 1) was determined using the methodology of Ward (1994) was compiled from data presented by Kahle et al. (2000) for the 1981 to 1998 time period. Measured slip rates presented by Awata et al. (2003) are compared to geodetic moment rate. The map provides a view of pre-earthquake strain associated in part with the time interval evaluated in this study. Maximum strain is narrowly distributed along the central part of the rupture zone (Golcuk and Tepetarla segments) and is greater across wider areas to the east and west.

Geodetic moment rate (1981-1998) rises linearly, west-to-east, along the Izmit-Sapanca fault from Golcuk into the Aksu segments. Within the Aksu segment moment rate drops abruptly, east of longitude 30.8 degrees (Figure 1). The pattern of measured slip (see Figure 1, from Awata et al., 2003) is non uniform. The characteristics of slip along the Izmit-Sapanca fault can be described as approximately constant along the Tepatarla segment at about 300cm (dextral), as dropping from nearly 500 cm to 0 (west to east) along the Arifiye segment, and as approximately constant at 100cm across the Aksu segment (Figure 1). Lake Sapanca and the Akyazi Gap mark the locations of abrupt changes in net slip along the Izmit-Sapanca fault.

2. Data

In recent years, a large number of seismographs have been added to the seismological networks (MARNET and IZINET) that monitor the Marmara (Evans et al., 1982; Evans et al., 1985; Ucer et al., 1985) and Izmit regions (Ito et al., 2002),

respectively. Errors in epicenter location and depth are estimated to be 1.8 km with a standard error of ± 1.1 km and 3.4 km with a standard error of ± 3.6 km, respectively (Akihiko Ito, 2004,Personal communication). Given the larger errors in depth, the estimates of spatial fractal dimension (D_S) were derived from the epicenter distribution rather than the hypocenter distribution. Errors in spatial location have no effect on the estimates of the temporal fractal dimension (D_T). The increased station density yielded considerable improvement in the quality of data recorded by these networks. The MARNET and IZINET networks have contributed significantly to a better understanding of crustal heterogeneity and fault activity in this area of northwestern Turkey (Ito et al., 2002; Ucer et al., 1985). Several major cities including Istanbul are located in this high seismic risk region. Recent improvements to the networks provide increased sensitivity that is critical to the accurate measurement of changes in the frequency, magnitude, and distribution of earthquakes in the region (Öncel et al., 1995; Oncel and Wyss, 2000a; Oncel and Wyss, 2000b).

The geographic extent of the earthquake slip area lies between longitudes of 29°-31° E and latitudes of 40.5°-41° N (see Figure 1). Although data evaluated in this study span the January, 1991 through June of 1999 time interval, the requirement that individual analysis windows contain at least 100 events resulted in average times that extended from 1991.95 to 1998.24. Analysis of declustered seismicity compiled from the MARNET catalogue in the region conducted by Öncel and Alptekin (1999) reveals a magnitude shift of 0.3 and change in the completeness magnitude (M_c) in 1990 from 2.6 (1981-1989) to 2.9 (1990-1998) after shift correction (see also Oncel and Wyss, 2000a). Analysis of data restricted to this time interval avoids the artificial influences on

seismicity rate associated with changes in the seismograph array that occurred prior to 1990. Temporal changes in *b* value and the generalized fractal dimension (D_q) were estimated for sliding windows whose duration was varied to contain 100 consecutive events. Consecutive windows were advanced through time by 10 event increments to provide a time-series representation for each of these seismotectonic variables.

3. Method

a) b-value and event rate (N)

The Gutenberg and Richter (1954) relation:

$$\text{Log}N = a - bM \quad (1)$$

implies a fractal relation between earthquake frequency and magnitude. Fractal behavior extends to the distribution of radiated energy, seismic moment, and fault length through their interrelationship to magnitude. The *b* value is widely used to describe the size scaling properties of seismicity. N is seismic event rate and the log (N) is linearly related to earthquake magnitude (M). The magnitude used in the present study is the duration magnitude (M_D). M_D is the most common magnitude reported by the Turkish seismic networks operated by Kandilli Earthquake Research Institute (KOERI). M_D is believed to be a more reliable measure of background seismicity because of saturation problems associated with other magnitude measures (e.g. M_L and M_B) (Castellaro et al., 2005). The intercept (*a*) provides a measure of background seismicity. Shaw et al., (1992) suggest that variations in *a* may also have predictive value. The slope (*b* value) defines

the change in occurrence rate with magnitude. Only events having magnitude ≥ 2.9 were used in this study.

The event rate (N) for each 100-event time window is

$$N=n/T=10^{a}, \quad (2)$$

where n=100 and T is the duration of the 100 event time window, and *a* is the intercept.

The *b* -value was estimated using the maximum likelihood method (Aki, 1965)

$$b=2.303/(M_{mean}-M_{min}+0.05), \quad (3)$$

where M_{mean} is the mean magnitude of events with $M>M_{min}$, and M_{min} (2.9) is the minimum magnitude of completeness in the earthquake catalogue. The maximum likelihood method is considered to provide a least biased estimate of *b* value. Local scale estimates of *b* range from 1.5 to 2.26 in the present study and are larger than the estimates of 0.5< *b* <1.6 obtained from events of M>4.5 reported in previous analysis of seismicity in this region (Öncel et al., 1995). The value 0.05 in Equation 3) is a correction constant that compensates for round off errors. The 95% confidence limits on the estimates of *b* are $\pm 1.96b/\sqrt{n}$, where *n* is the number of earthquakes used to make the estimate. This yields 95% confidence limits of 0.16 ± 0.1-0.2 for sliding windows of n=100 earthquakes in this study.

b) Generalized fractal dimension

Following Grassberger and Procaccia, 1983, *Godano and Caruso*, 1995; *Lei and Kusunose*, 1999; *Smalley Jr et al.*, 1987; *Sunmonu et al.*, 2001, the generalized multifractal dimension, D_q, for epicenter distribution is defined as follows:

$$D_q = \frac{1}{(q-1)} \lim_{r \to 0} \frac{\log \sum C(r)_i^q}{\log r} \quad (4)$$

where q, in this study, is varied from 2 to 15, and C (r) is the correlation integral

$$C_q(r) = \frac{1}{N}\left[\sum_{i=1}^{N}\left(\frac{N_j(R \le r)}{N-1}\right)^{q-1}\right]^{1/(q-1)} . \quad (5)$$

N is the number of points within a distance *r* of point *j* (*Smalley Jr et al.*, 1987; *Shah and Labuz.,* 2000; *Sunmonu et al.*, 2001) and *R* is varied from 0 to *r*. $C_q(r)$ gives the average fraction of epicenters within a radius *r* (Baker and Golub, 1990). Equations 4) and 5) specify the spatial characteristics of the epicenter distribution. Temporal variability can be estimated in a similar manner:

$$C_q(t) = \frac{1}{N}\left[\sum_{i=1}^{N}\left(\frac{N_j(T \le t)}{N-1}\right)^{q-1}\right]^{1/(q-1)} , \quad (6)$$

where $C_q(t)$ represents the the average fraction of epicenters that fall within a time window of size *t*. In Equation 4) we replace *r* with *t.* The multifractal parameter *q* was varied from 2 to 15. Multifractal dimensions D_q are estimated from the slope of the linear region of the log (C_q) versus log (r) plot in space and the slope of the linear region of the log (C_q) versus log (t) plot in time. Linearity in the relationship between log (C_q) and log (r) [or log (t)] implies a power law or fractal relationship between C_q and r [or t]. In this expression, C_q(r or t) is the number of event pairs occurring in the space range R<r or in the time range T<t. The linear range in the log(C_q) versus log (r) or log(t) plots is specified by r_{min} and r_{max} in space, and t_{min} and t_{max} in time. Edge effects associated with saturation (at small r or t) and depopulation (at large r or t) are avoided.

We computed D_q (S and T) over a fixed range of distances and times corresponding to 7-60 km and 0.04-1.51 yr, respectively. Examples of log (C) vs. log (r) plots (Figures 2a and b) immediately preceding the Izmit event reveals linear behavior

over a limited range of r and t. Note that multifractal dimensions decrease with increasing q and that D_T is less than D_S for all values of q (Figure 2c). The variation of D with q arises from heterogeneity in multifractal patterns of clustering in time and space. The mean standard error for D_S (q=2) is ± 0.03 (with range from 0.01-0.05); for q = 15, the standard error is ±0.02 (with range from 0.01-0.05). Mean standard errors for time fractal dimensions (D_T) are ± 0.02 (0.02-0.04) for q=2, and ± 0.04 (0.02-0.08) for q=15.

4. Observations and Relationships

- ***b* value, Magnitude, and Event Rate**

In the 7 year interval preceding the Izmit event, the *b* value fluctuated from a high of 2.1 in 1992.5 to a low of 1.6 in 1995 and then rose to an even higher value of 2.25 in early 1998 (see Figure 3a and 4). Changes in mean magnitude through this same time period (Figure 3a) correlate inversely with *b* value as expected from Equation 3.

The relationship of event rate to changes of *b* value also varied through time (see Figure 3 and 4). From 1992.13 to 1993.4 (average times) log(N) is negatively correlated to *b* (-0.62), while from 1995.4 to 1998.4 the correlation becomes positive (r = 0.85) (see Figure 4). Log (N*)* increases to a maximum in 1997.7 and then decreases preceding the Izmit event. During the entire 8 year period of analysis, earthquake frequency remained relatively constant until mid-1996 when it began to increase steadily. A slight drop in frequency occurred 1.5 years prior to the Izmit event.

- **Interrelationships between Temporal and Spatial Fractal Dimensions**

Spatial variations of D_2 and D_{15} through the period of analysis are highly correlated (r = 0.99). The correlation dimension (D_2) is significantly greater than the other multifractal dimensions (i.e., q = 3 to 15) and varies from 0.7 to 1.22 (Figure 3c). D_{15} (S) varies from

0.44 to 1. These observations suggest, as we would expect, that seismicity is more clustered at local scales defined by D_{15} than at more regional scales defined by D_2. Temporal values of multifractal dimension (Figure 3d) vary from approximately 0.65 to 0.85 at regional scale (i.e. q = 2) and from approximately 0.3 to 0.6 at local scale (q = 15). Median values of $D_2(T)$ and $D_{15}(T)$ through the period of analysis are less than 1 (0.7 and 0.5, respectively). Values of $D_T < 1$ are indicative of clustering; whereas $D_T > 1$ is associated with more dispersed and randomly distributed hypocenter distributions (*Kagan and Jackson*, 1991).

Correlation between temporal ($D_2(T)$) and spatial clustering ($D_2(S)$) oscillates from positive to negative (Figure 5b). There are three periods of positive correlation between $D_2(S)$ and $D_2(T)$ peaking in 1993, mid 1995 and late 1997. Variations in r are evaluated in terms of the probability (p value) that these correlation coefficients could actually be 0 or have opposite sign. Using a cutoff probability of 0.05, two of these positive correlations can be considered significant: one with p value of 0.005 (late 1992) and the other with p value of 0.01 (late 1997). The positive correlation in 1995 is not significant. The variations in D_2 from late 1993 on, are relatively minor, and generally parallel each other (Figure 5a). Periods of negative correlation (early 1994 and 1996) are not significant. The positive correlations are associated with increasingly clustered seismicity in time and space (1992 through mid 1993) or small decreases in time-space clustering during the later part of the observation period (1996 to mid 1998).

The correlations between $D_{15}(S)$ and $D_{15}(T)$ differ somewhat from those between $D_2(S)$ and $D_2(T)$ (Figure 5d). Two periods of significant positive correlation appear at local (q = 15) scale. The tail-end of a period of positive correlation is observed in early

1993 and an extended period of positive correlation continues from about mid-1995 till the end of the time series with mean time of 1997.6. The early positive correlation is associated with a parallel decrease in D_{15}, while the extended period of positive correlation is associated generally with parallel increases in D_{15}. Overall, time-space variations in D_2 and D_{15} are fairly similar. Both are characterized by periods of increased clustering (drop in D) during the 1992 to mid 1993 time period. Toward the end of the observation period (mid 1998), increases of D associated with increasingly dispersed seismicity are accompanied by a period of anomalously low magnitude seismicity and increased event rate (Figure 3a and 3b respectively).

- **Statistical Comparisons**

Detailed statistical comparisons of temporal and spatial variations in D (Figure 5) and variations of *b* and D_2 (S) (Figure 6) for the 8 year period preceding the Izmit event reveal complex short-term variability. In each comparison, correlation coefficients were computed for consecutive intervals containing 8 time steps. The time steps are variable because parameters were computed for windows containing 100 seismic events and the center of each window was separated from the next by 10 events. The time associated with each point (Figures 5 and 6) is the average time for the data contained in each 8-point window. On average, the correlations are computed at 0.25 year intervals. While significant overlap in the data from one window to the next ensures similar correlation between consecutive time windows, consistent long-term correlation differences are present. The probability (p) that these correlation coefficients could actually be zero or have opposite sign is also plotted as an indication of the reliability of the correlation coefficient (Figures 5 and 6). P values ≤ 0.05 indicate that significant positive and

negative correlations are present. As expected, the correlations become insignificant (p values become greater than 0.05) during phase transitions as the correlation coefficients change from positive to negative or vice versa.

- **Phase Changes and Variations in Strain Distribution**

The relationship between *b* and D_2(S) (Figure 6) reveals three phases of significant correlation (p approximately equal to zero) referred to as Phase I, II, and III (see also Figure 3). Phase I represents a period of positive correlation that extends from late 1992 through mid 1994.4 (Figures 6b and 7). A second period of positive correlation (Phase III) extends from mid 1996 through mid 1998. The interval of time between these two periods is associated primarily with the transition from positive to negative correlation and back again. The intervening period of negative correlation (Phase II) is interpreted to extend approximately from 1994.4 through mid 1996 and includes the transition periods (Figures 6 and 7).

The interrelationships between *b* and D_2(S) that lead to positive and negative correlation are portrayed in Figure 7. Periods of positive correlation occur in two different ways. The first positive correlation period (Phase I) is associated with a period during which *b* and D_2(S) decline together (1992 to1994.4, Figure 7). These changes are associated with clustering of higher magnitude seismicity and suggest that seismic strain is more concentrated. Earthquake magnitude averages about 3.1 during this phase. A second period of positive correlation between D_2(S) and *b* returns in 1997 (Phase III). This phase is associated with a large increase in *b* value (see Figure 3a), a substantial growth in seismicity rate (Figure 3b) and increases in D_2(S). The average magnitude during Phase III drops to approximately 3.04 and does not fall in the category of

intermediate magnitude earthquakes that Jaume and Sykes (1999) note sometime precede a major earthquake. Phase III behavior is suggestive of the negative feedback process (Henderson and Main, 1992) in which there is an absence of interaction between distributed fault segments. The rapid increase of *b* and log (N) suggest that slip is beginning to occur on smaller segments of the Izmit-Sapanca fault. During Phase III, *b* and $D_2(S)$ rise together. Seismicity becomes less clustered, rising approximately from 0.6 to 0.9 (see Figures 6 and 7); however, it remains relatively concentrated with $D_2(S) < 1$. The negative correlation period (Phase II) is associated with an increase in b (dropping magnitude) followed by a decrease in $D_2(S)$ (increased clustering) extending from approximately mid 1994 through mid 1996 (Figure 7). Associated earthquake magnitude drops (b increases). Overall, these changes suggest that strain release becomes increasingly clustered on smaller fault segments a few years preceding the Izmit event. The pattern of maximum strain distribution along the fault zone also suggests that this is the case (Figure 1). Maximum strain is less along the central portion of the rupture zone and the magnitude of maximum strain in this region is narrower than to the east and west.

5. Discussion of Observations

The steady increase in *b* value in the two-year period preceding the Izmit event is similar to that observed prior to rupture of laboratory scale rock fracture experiments (Henderson et al., 1994; Lei et al., 2000; Main et al., 1989; Smith, 1986). In their experiments *b* value associated with microseismicity in core samples increased to approximately 2 prior to failure.

Anomalous variations in *b* value often occur prior to major earthquakes. *Fiedler* (1974) and *Smith* (1981 and 1986) reported intermediate-term increases of *b* value preceding large earthquakes in New Zealand associated with dip slip fault displacements. *Smith* (1981) also suggested that this attribute could be characterized by a parameter he called the total precursor time (T). Smith computed the precursor time from magnitude using the relationship Log T (days) =1.42+0.30 M (see Table 1 of *Smith* 1981). Using M_D=6.8 (M_w=7.4) for the Izmit event yields a precursor time of 7.9 years. This is considerably longer than the 4 to 5 year rise time preceding the Izmit event. *Smith*'s [1981] precursor time is derived for earthquakes associated with thrust faults. Precursor times along strike-slip faults such as the Izmit Sapanca fault may be intrinsically different.

Main and Meredith (1989) note the presence of critically low values of *b* (approximately 0.5) preceding the Western Nagano earthquake of 1984. At Nagano, decreasing *b* value was accompanied by periods of seismic quiescence. In their study, laboratory experiments revealed similar decreases in *b* value prior to rupture. *Main and Meredith* (1989) indicate, however, that the drop in *b* value by itself is not sufficient to issue high-level warnings, noting that a similar drop of *b* value was observed in 1983 which gave rise to a false alarm in the Nagano area. Jaume and Sykes (1999) also report decreased *b* values associated with an increased frequency of intermediate magnitude events (generally M>5.0) preceding large or great earthquakes (M>6.5-7.0). The size of the region associated with these earthquakes scales in proportion to the magnitude of the subsequent main shock suggesting that D(S) would increase during this phase. The analysis of Karakaisis (2003) reveals a period of decreasing *b* value from 1981 to 1996. This stands in contrast to the results of Oncel and Wilson (2002) which reveal general

increases in *b* along the western segment of the Northern Anatolian Fault Zone (Figure 8). The work of Karakaisis (2003) includes all of western Turkey in the analysis of *b* value variation. Since this region includes a major strike slip zone, a zone of extension in west-central Turkey, and a zone of compression to the south, it does not isolate behavior associated with the Izmit fault zone.

These contrasting observations may be associated with differences in the ability to resolve variations over short time intervals. The observations of *Main et al.* (1989) revealed that *b* value preceding the 1984 Western Nagano event increased from a low about 0.6 (approximately 2 years prior to the event) to 1.2 about 4 months prior to the event. The *b* value then dropped rapidly from 1.2 to 0.6 during the 4 month period immediately preceding the event. The earlier rise in *b* value was suggested by Main et al. (1989) to result from diffusion of pore fluids into the fault zone and reduced pore pressure (see Figure 3 of Main et al., 1989). The periods during which b value dropped were associated with pore pressure increase and seismic quiescence. If the numbers of events exceeding the threshold magnitude are not sufficient to allow statistically significant estimates of *b* value over such short time frames, the drop in *b* value may not be observed. In *Vinciguerra*'s (2002) analysis of seismicity preceding the 1989 eruption of Mt. Etna, a sudden drop in *b* value was also observed. The abrupt drop of *b* occurred over a few days ending an approximately 3 month long period of gradually dropping or constant *b*. At the time of eruption *b* dropped to approximately 0.5 similar to that observed by *Main and Meredith* (1989).

It has been argued that the upper limit of the *b* value should theoretically not exceed 1.5 (see *Olsson*, 1999). The *b*-value of global seismicity derived from larger

moment magnitude events is approximately 1.0 (e.g., *Kagan*, 1994). The *b* values observed along the Izmit-Sapanca fault exceed 2.2 for a short time and are generally greater than 1.5. At more local scales *b* varies from 0.5 to 1.6 (e.g., *Oncel and Wyss*, 2001). The *b* values observed by *Main and Meredith* [1989] in the 5-year period preceding the Western Nagano event reached a maximum of only 1.4. Observational data, however, suggest that *b* values as large 2.2-2.5 may be observed (*Smith*, 1986; *Westerhaus et al*., 2002; *Henderson et al*., 1992). Similar results are also obtained from experimental seismology (*Lei et al*., 2000). The discrepancies between theory and observation may be associated with distinctions between micro and macro-seismicity (*Kagan*, 1994). We observed a maximum *b* value of 2.25 similar to that observed by Henderson et al. (1992) preceding the 1983 Coalinga earthquake near Parkfield (M=6.7). We did not observe the increase in *b* value and intermediate magnitude seismicity reported by Jaume and Sykes (1999).

The analysis of D_q reveals an early period (Phase I) where D is high and seismicity is dispersed ($D_2 > 1$). D (S and T) are significantly lower during Phases II and III. At the end of Phase I we see a rapid transition to clustered seismicity about 6 years preceding the Izmit event, and a drop in magnitude (increased *b*). About 3 years prior to the Izmit event (beginning of Phase III), seismicity becomes gradually less clustered, while *b* continues to increase.

6. Conclusions

We analyzed seismicity in the region surrounding the Izmit Sapanca fault during a 7.4 year period (1991 to 1998.4) preceding the 1999 Izmit event (M_D = 6.8 or M_w=7.4).

The study area lies in northwestern Turkey between 40.5^{o} to 41^{o} north latitude, and 29^{o} and 31^{o} east longitude. Seismic events during this time were subdivided into smaller overlapping time intervals for analysis and comparison.

The correlation between *b* and D varied from significantly positive to negative and back again during the analysis period. Oscillations in *b* value have been reported by others (see Main and Meredith, 1989; Henderson and Main, 1992; and Vinciguerra, 2002). The results of this study reveal anomalous behavior in the intermediate-term seismicity preceding the Izmit event. Phase III seismicity, approximately 1.5 to three years preceding the event, remained clustered, and was characterized by a rapid rise in *b* from 1.6 to 2.26. Over the long-term (approximately 50 years), fluctuations in *b* value reached higher and higher peaks (Figure 8). In western Turkey, *b* value rose from 1.6 in 1974 to 2.1 in 1992 and then to 2.26 in 1998. We are missing the details of these variations from 1985 to 1992 and for the 1.5 years immediately preceding rupture. A similar increase is observed in the years leading up to the Coalinga earthquake (Henderson et al., 1992). Examination of data presented by Henderson et al. (1992) shows that oscillations in *b* value reached their highest value about 3 months preceding final rupture. The *b* value rose to maxima of 1.8 and 1.85 in 1973 and 1976 respectively, before rising to approximately 2.25 prior to the Coalinga event.

Concentration of strain along the rupture zone appears to be a long-term characteristic of the Izmit-Sapanca fault segment from 1981 to 1998 leading up to final rupture (see Figure 1). This also corresponds to a time during which D was close to or less than 1 (thus relatively clustered) and during which *b* increased from about 1.1 to 2.26. The final period of anomalous behavior preceding the Izmit event (Phase III) is

associated with accelerated low magnitude seismicity ((increasing *b* value) during which seismicity becomes more dispersed but remains relatively clustered with (D <1). This behavior is similar to the negative feedback process described by Henderson and Main (1992) in which strain release becomes increasingly dispersed while event magnitude drops. At Izmit, rupture appears to occur on faults with smaller and smaller surface area during this phase. Henderson and Main (1992) observe a period of positive feedback in which faults begin to coalesce leading to larger magnitude events. We do not observe this phenomenon; however, we suspect that the period of accelerated seismicity associated with Phase III eventually led to coalescence of fault surfaces and final rupture. We did not see the drop in *b* value often reported to precede a major event. This drop, if it occurred, appears to have been fairly abrupt in the case of the 1999 Izmit event. Data presented by Henderson and Main (1992) for the Coalinga earthquake near Parkfield, California, indicate that this drop can be quite sudden, appearing only two to three months prior to rupture. The frequency of earthquake occurrence may not permit a statistically accurate short term estimate of the *b* value. In cases where the number of observed events preceding main rupture is too low to resolve the drop in *b* value, cycles of accelerated low magnitude seismic activity in which *b* becomes anomalously high (>2) may serve as an early warning of an impending large magnitude rupture.

Acknowledgements.

We appreciate the comments of Dr. Ian Main. Appreciation is also extended to Dr. Xinglin Lei who provided use of his software to determine multifractal dimensions. AO also appreciate partial funding of his research through Japan AIST fellowship.

References

Aki, K., Maximum likelihood estimate of b in the formula logN=a-bM and its confidence limits, *Bulletin Earthquake Research Institute of Tokyo University*, *43*, 237-239, 1965.

Awata, Y., T. Yoshioka, O. Emre, T. Duman, A. Dogan, E. Tsukuda, M. Okamura, H. Matsuoka, and I. Kuscu, Outline of the surface rupture of 1999 Izmit earthquake, in *Surface rupture associated with the August 17, 1999 Izmit earthquake*, pp. 41-50, MTA, Ankara, 2003.

Baker, G., and Gollub, J., 1990, Chaotic Dynamics: an Introduction: Cambridge University Press, 182p.

Castellano, 2005

Evans, R., I. Asudeh, S. Crampin, and B. Ucer, Microtectonics in the Marmara Sea Region, *Geophysical Journal of the Royal Astronomical Society*, *69* (1), 284-284, 1982.

Evans, R., I. Asudeh, S. Crampin, and S.B. Ucer, Tectonics of the Marmara Sea Region of Turkey - New Evidence from Micro-Earthquake Fault Plane Solutions, *Geophysical Journal of the Royal Astronomical Society*, *83* (1), 47-60, 1985.

Fielder, 1974

Godano, C., and V. Caruso, Multifractal Analysis of Earthquake Catalogs, *Geophysical Journal International*, *121* (2), 385-392, 1995.

Grassberger, P., and I. Procaccia, Measuring the strangeness of strange attractors, *Physica 9D*, 189-208, 1983.

Gutenberg, B., and C.F. Richter, *Seismicity of the Earth and Associated Phenomena*, Princenton University Press, Princeton, 1954.

Henderson, J., and I. Main, A Simple Fracture-Mechanical Model for the Evolution of Seismicity, *Geophysical Research Letters*, *19* (4), 365-368, 1992.

Henderson, J., I. Main, P.G. Meredith, and P.R. Sammonds, The evolution of seismicity at Parkfield:observation, experiment and a fracture-mechanical interpretation, *Journal of Structural Geology*, *14*, 905-913, 1992.

Ito, A., B. Ucer, S. Baris, A. Nakamura, Y. Honkura, T. Kono, S. Hori, A. Hasegawa, R. Pektas, and A.M. Isikara, Aftershock activity of the 1999 Izmit, Turkey, earthquake revealed from microearthquake observations, *Bulletin of the Seismological Society of America*, *92* (1), 418-427, 2002.

Jaume and Sykes (1999)

Kahle, H.G., M. Cocard, Y. Peter, A. Geiger, R. Reilinger, A. Barka, and G. Veis, GPS-derived strain rate field within the boundary zones of the Eurasian, African, and Arabian Plates, *Journal of Geophysical Research-Solid Earth*, *105* (B10), 23353-23370, 2000.

Kagan, Y.Y. and Jackson, D.D., 1994. Long-Term Probabilistic Forecasting of Earthquakes. Journal of Geophysical Research-Solid Earth, 99(B7): 13685-13700.

Karakaisis, G.F., 2003. Accelerating seismic crustal deformation before the Izmit earthquake (NW Turkey) large mainshock of 1999 August 17 and the evolution of its aftershock sequence. Geophysical Journal International, 153: 103-110.

Kostrov, B.V., Seismic moment and energy of earthquakes and seismic flow of rock, *Izvestiya-Physics of the Solid Earth*, *1*, 23-40, 1974.

.

Lei, X.L., and K. Kusunose, Fractal structure and characteristic scale in the distributions of earthquake epicentres, active faults and rivers in Japan, *Geophysical Journal International*, *139* (3), 754-762, 1999.

Lei, X.L., K. Kusunose, M.V.M.S. Rao, O. Nishizawa, and T. Satoh, Quasi-static fault growth and cracking in homogeneous brittle rock under triaxial compression using acoustic emission monitoring, *Journal of Geophysical Research-Solid Earth*, *105* (B3), 6127-6139, 2000.

Main, I., Statistical physics, seismogenesis, and seismic hazard, *Reviews of Geophysics*, *34* (4), 433-462, 1996.

Main, I.G., P.G. Meredith, and C. Jones, A reinterpretation of the precursory seismic b-value anomaly from fracture mechanics, *Geophysical Journal International*, *96*, 131-138, 1989.

Main, I., and P.G. Meredith, Classification of earthquake precursors from a fracture mechanics model, *Tectonophysics*, *167*, 273-283, 1989.

Nakaya, S., and T. Hashimoto, Temporal variation of multifractal properties of seismicity in the region affected by the mainshock of the October 6, 2000 Western Tottori Prefecture, Japan, earthquake (M=7.3), *Geophysical Research Letters*, *29* (10), art. no.-1495, 2002.

Olsson, R., 1999. An estimation of the maximum b-value in the Gutenberg-Richter relation. Geodynamics, 27: 547-552.

Öncel, A.O., and Ö. Alptekin, Microseismicity of Marmara Sea and Seismic Hazard, pp. 40, Research Foundation of Istanbul University, 1999.

Öncel, A.O., Ö. Alptekin, and I. Main, Temporal variations of the fractal properties of seismicity in the western part of the northAnatolian fault zone:possible artifacts due to improvements in station coverage, *Nonlinear processes in Geophysics*, *2*, 147-157, 1995.

Oncel, A.O., I. Main, O. Alptekin, and P. Cowie, Temporal variations in the fractal properties of seismicity in the North Anatolian Fault Zone between 31 degrees E and 41 degrees E, *Pure and Applied Geophysics*, *147* (1), 147-159, 1996.

Oncel, A.O., and T.H. Wilson, Space-time correlations of seismotectonic parameters: Examples from Japan and from Turkey preceding the Izmit earthquake, *Bulletin of the Seismological Society of America*, *92* (1), 339-349, 2002.

Oncel, A.O., and M. Wyss, The major asperities of the 1999 M-w=7.4 Izmit earthquake defined by the microseismicity of the two decades before it, *Geophysical Journal International*, *143* (3), 501-506, 2000a.

Oncel, A.O., and M. Wyss, Mapping the major asperities by minima of local recurrence time before the 1999 M7.4 Izmit earthquake, in *The Izmit and Duzce Earthquakes: preliminary results*, pp. 1-14, Istanbul Technical University, Istanbul, 2000b.

Oncel, A.O. and Wilson., T., 2004. Correlation of seismotectonic variables and GPS strain measurements in western Turkey and the eastern Mediterranean. in preparation.

Oncel, A.O. and Wyss, M., 2000. The major asperities of the 1999 M-w=7.4 Izmit earthquake defined by the microseismicity of the two decades before it. Geophysical Journal International, 143(3): 501-506.

Scholz, C.H., 2002. Earthquakes and Faulting. Cambridge University Press, 471 pp.

Shah, K.R. and Labuz, F.J., 1995. Damage mechanisms in stressed rock from acoustic emission. Journal of Geophysical Research-Solid Earth, 100: 15,527-15,539

Shaw, B.E., Carlson, J.M. and Langer, J.S., 1992. Patterns of seismic activity preceeding large earthquakes. Journal of Geophysical Research Astronomical Society, 97: 479-488.

Shaw, B.E., 1993. Generalized Omori law for aftershocks and foreshocks from a simple dynamics. Geophysical Research Letters, 20: 907-910.

Smalley Jr, R.F., J.L. Chatelian, D.L. Turcotte, and A. Prevot, A fractal approach to the clustering of earthquakes: Applications to the seismicity of New Hebrides, *Bulletin Seismological Society of America*, *77*, 1368-1381, 1987.

Smith, D.W., The b-value as an earthquake precursor, *Nature*, *289*, 136-139, 1981.

Smith, D.W., Evidence for precursory changes in the frequency-magnitude b-value, *Geophysical Journal Royal Astronomical Society*, *86*, 815-838, 1986.

Steacy, S., and S. McClusky, Heterogeneity and the earthquake magnitude-frequency distribution, *Geophysical Research Letters*, *26* (7), 899-902, 1999.

Sunmonu, L.A., V.P. Dimri, M.R. Prakash, and A.R. Bansal, Multifractal approach to the time series of M >= 7.0 earthquake in Himalayan region and its vicinity during 1895-1995, *Journal of the Geological Society of India*, *58* (2), 163-169, 2001.

Toksoz, M.N., A.F. Shakal, and A.J. Michael, Space-Time Migration of Earthquakes Along the North Anatolian Fault Zones and Seismic Gaps, *Pure and Applied Geophysics*, *117*, 1258-1270, 1979.

Ucer, S.B., S. Crampin, R. Evans, A. Miller, and N. Kafadar, The Marnet Radiolinked Seismometer Network Spanning the Marmara Sea and the Seismicity of Western Turkey, *Geophysical Journal of the Royal Astronomical Society*, *83* (1), 17-30, 1985.

Vinciguerra, S., Damage mechanics preceding the September-October 1989 flank eruption at Mount Etna volcano inferred by seismic scaling exponents, *Journal of Volcanology and Geothermal Research*, *113*, 391-397, 2002.

Ward, S., A multidisciplinary approach to seismic hazard in southern California, *Bulletin Seismological Society of America*, *84* (5), 1293-1309, 1994.

Westerhaus, M., Wyss, M., Yilmaz, R. and Zschau, J., 2002. Correlating variations of b values and crustal deformations during the 1990s may have pinpointed the rupture initiation of the M-w=7.4 Izmit earthquake of 1999 August 17. Geophysical Journal International, 148(1): 139-152.

FIGURE CAPTIONS

Figure 1**.** a) Maximum GPS strain is shown in color, along with epicenter locations and fault displacement measurement points. b) Dextral slip and moment rate associated with the Izmit event are plotted along the length of the Izmit-Sapanca fault (*Awata et al*., 2003). Fault segments and seismic gaps are labeled for reference.

Figure 2. a) Temporal (logC(t) versus log(t in minutes)) and b) spatial (logC(r) versus log(r in km)) fractal plots are presented for multifractal dimensions q equal to 2 and 15. c) Variations of D(S) and D(T) are shown as a function of q.

Figure 3. Seismotectonic parameters evaluated in this study are presented together for comparison. a) *b* value and average magnitude for moving time windows; b) Log (N) (where $N=n/T_{obs}$ and n=100); c) and d) Spatial and temporal fractal dimensions D_2 and D_{15} are presented along with their standard errors. The plots are divided into three periods of behavior: phases I-III.

Figure 4. Variations of *b* value and event rate (log (N)) are compared for the 1992 through 1998.5 time period.

Figure 5. Comparisons of spatial and temporal correlation as a function of time are presented: a) $D_2(S)$ and $D_2(T)$; b) Correlation between $D_2(S)$ and $D_2(T)$ and associated p values; c) $D_{15}(S)$ and $D_{15}(T)$; d) Correlation between $D_{15}(S)$ and $D_{15}(T)$ and associated p values. Subdivisions corresponding to phases I through III are shown.

Figure 6: a) $D_2(T)$ and *b* value are compared during the 1992 to 1998.5 time interval. b) The correlation between D2(T) and b are followed through time. The p-value represents the probability that the correlation coefficient is significantly different from zero. Phases I through III associated with periods of positive and negative correlation are identified.

Figure 7. This figure illustrates the three different phases of behavior observed between b and D_2 (see also Figure 6). Phases I and III illustrate behavior during the periods of positive correlation observed in Figure 6. Phase II illustrates the relationship between b value and D_2 in the intervening period of negative correlation. Arrows on the regression lines indicate the direction of change occurring during each phase.

Figure 8. The long term relationship between *b* value and D is illustrated. Variations extending from 1945 through 1985 are derived from seismicity (M_S>4.5) along the western extension of NAFZ (24^oE to 31^oE; length≈695km) (see Oncel and Wilson, 2002). Variations shown from 1992 through 1998.5 are from the present study are extending from longitudes 29^oE to 31^oE (approximate length of 170km).

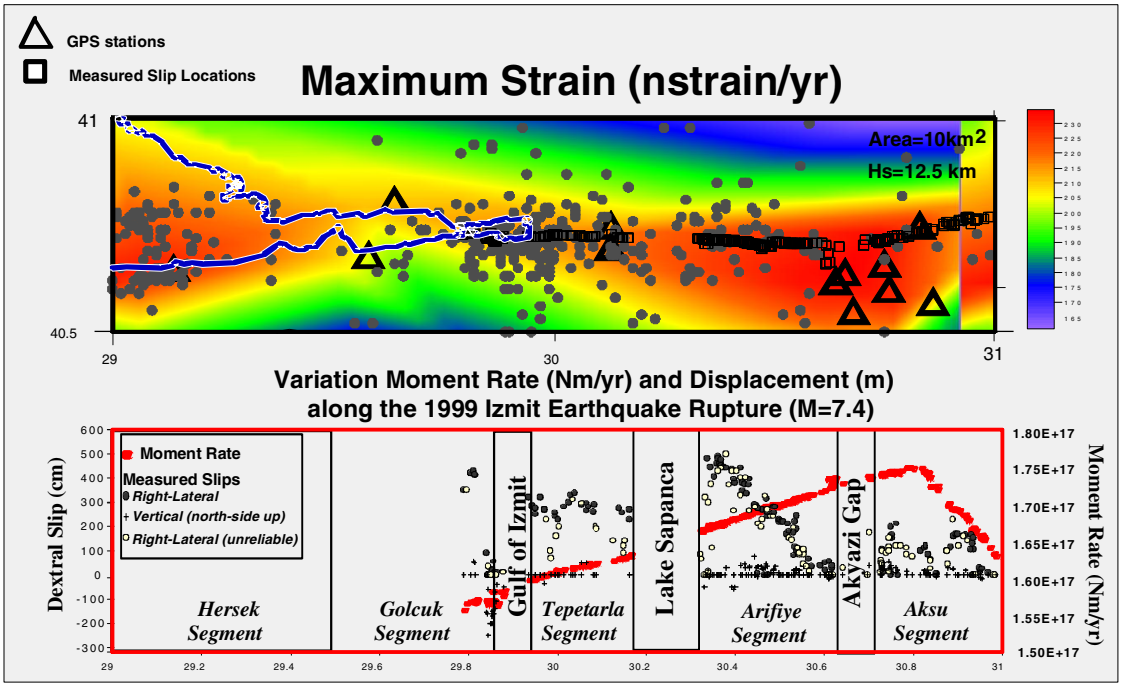
GPS stations
Measured Slip Locations
Maximum Strain (nstrain/yr)
Area=10km2
Hs=12.5 km
41
40.5
29
30
31
Variation Moment Rate (Nm/yr) and Displacement (m)
along the 1999 Izmit Earthquake Rupture (M=7.4)
Moment Rate
Measured Slips
Right-Lateral
Vertical (north-side up)
Right-Lateral (unreliable)
Dextral Slip (cm)
Moment Rate (Nm/yr)
Hersek Segment
Golcuk Segment
Gulf of Izmit
Tepetarla Segment
Lake Sapanca
Arifiye Segment
Akyazi Gap
Aksu Segment

Figure 1.

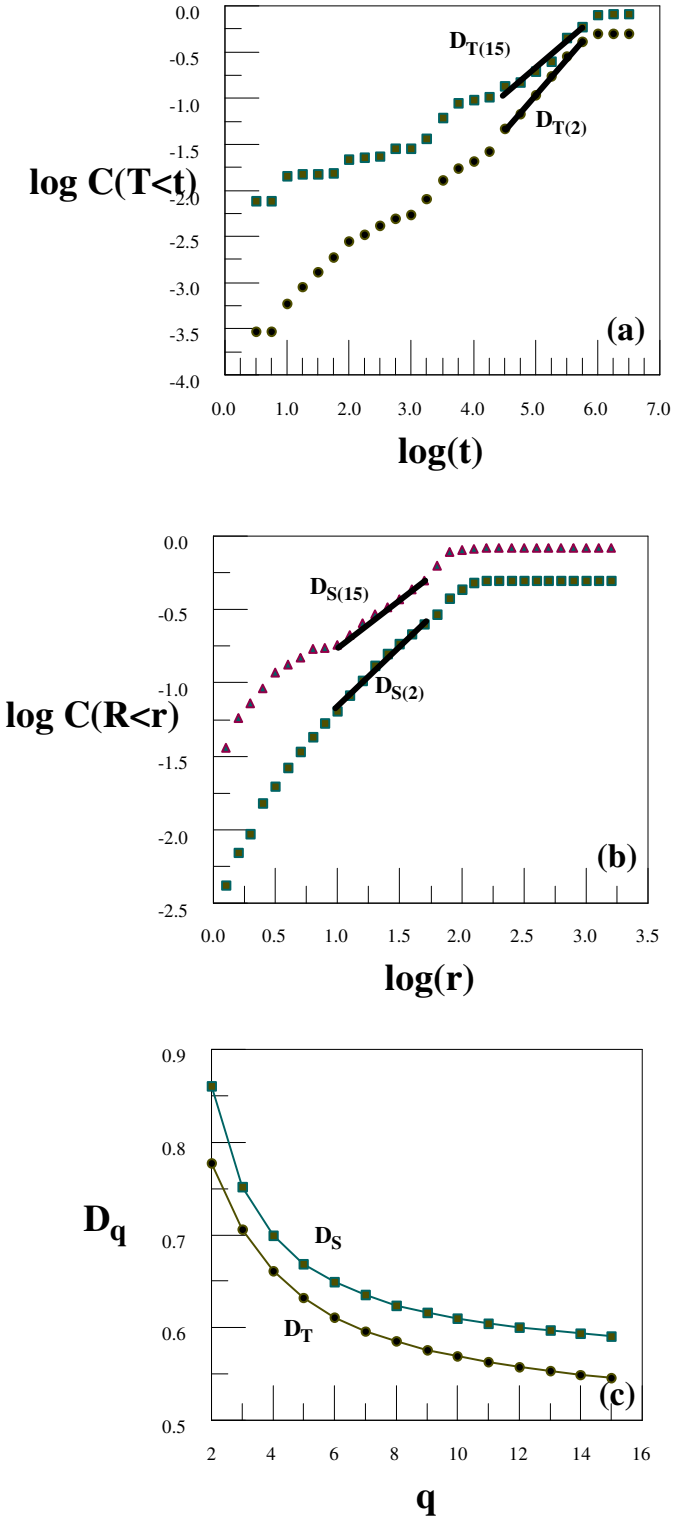

Figure 2.

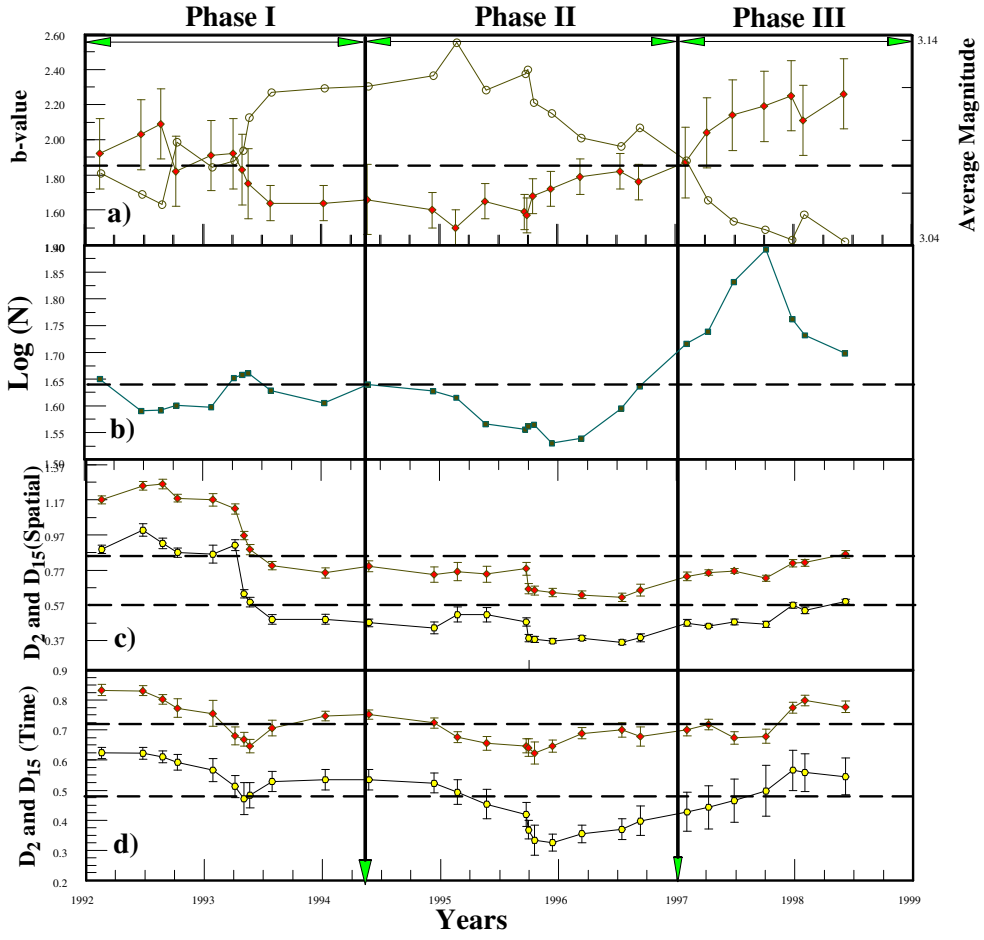
Phase I
Phase II
Phase III
b-value
Average Magnitude
a)
Log (N)
b)
D_2 and D_{15}(Spatial)
c)
D_2 and D_{15} (Time)
d)
Years

Figure 3

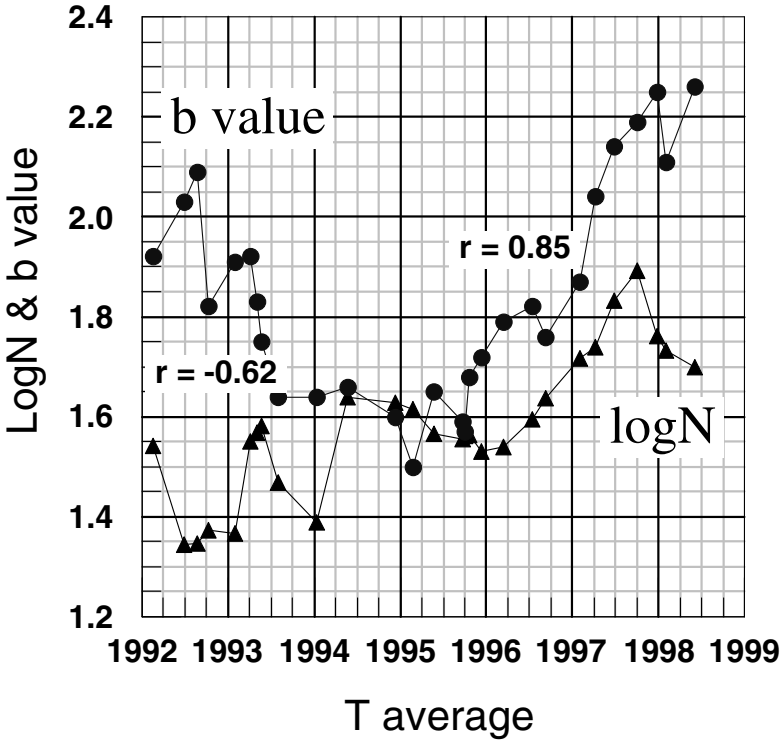
2.4
2.2
2.0
1.8
1.6
1.4
1.2
LogN & b value
b value
r = 0.85
r = -0.62
logN
1992 1993 1994 1995 1996 1997 1998 1999
T average

Figure 4

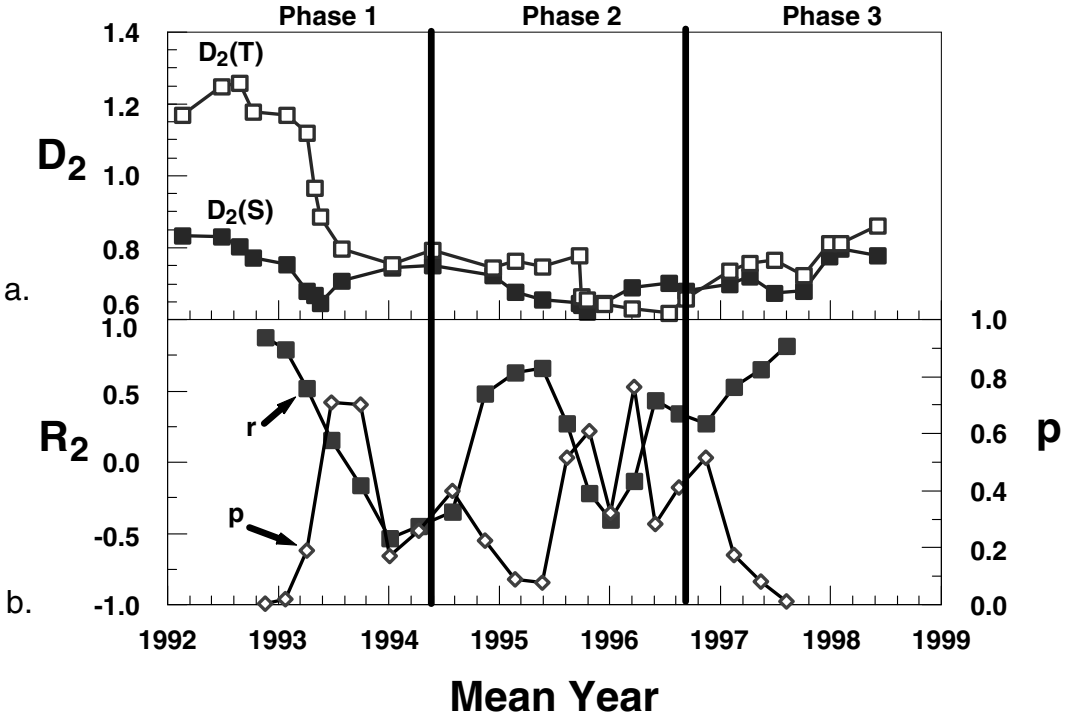
Phase 1
Phase 2
Phase 3
a.
b.
D2
D2(T)
D2(S)
R2
r
p
p
1.4
1.2
1.0
0.8
0.6
1.0
0.5
0.0
-0.5
-1.0
1.0
0.8
0.6
0.4
0.2
0.0
1992
1993
1994
1995
1996
1997
1998
1999
Mean Year

Figure 5ab

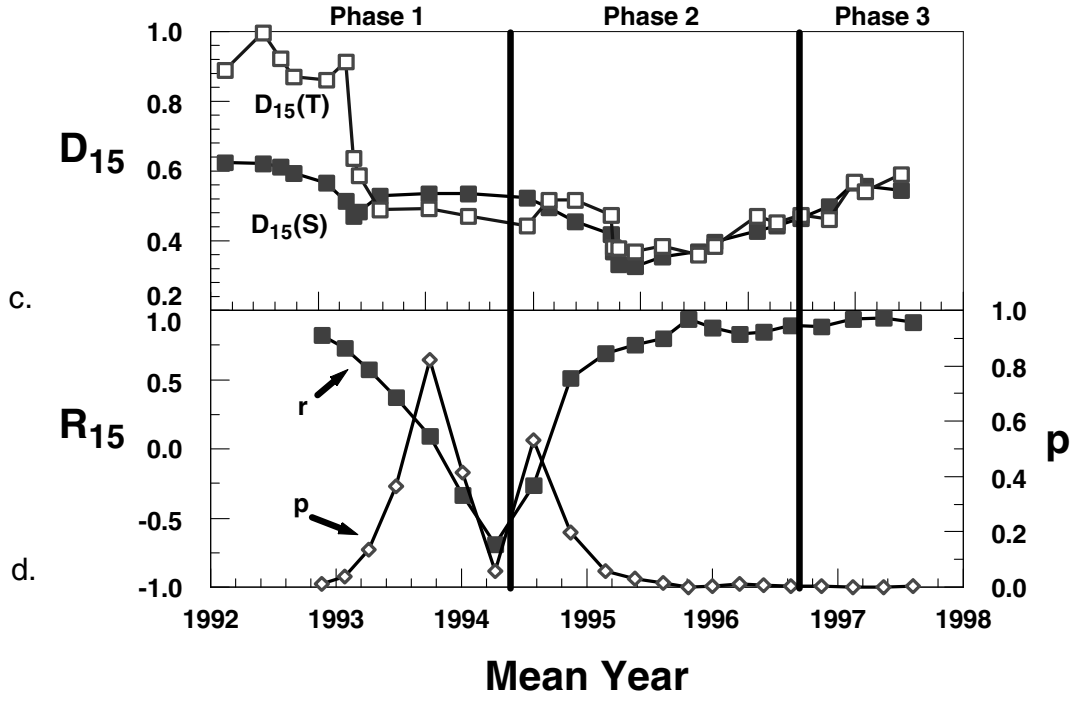
c.
d.
Phase 1
Phase 2
Phase 3
D15
D15(T)
D15(S)
R15
r
p
p
1.0
0.8
0.6
0.4
0.2
0.5
0.0
-0.5
-1.0
1992
1993
1994
1995
1996
1997
1998
Mean Year

Figure 5cd

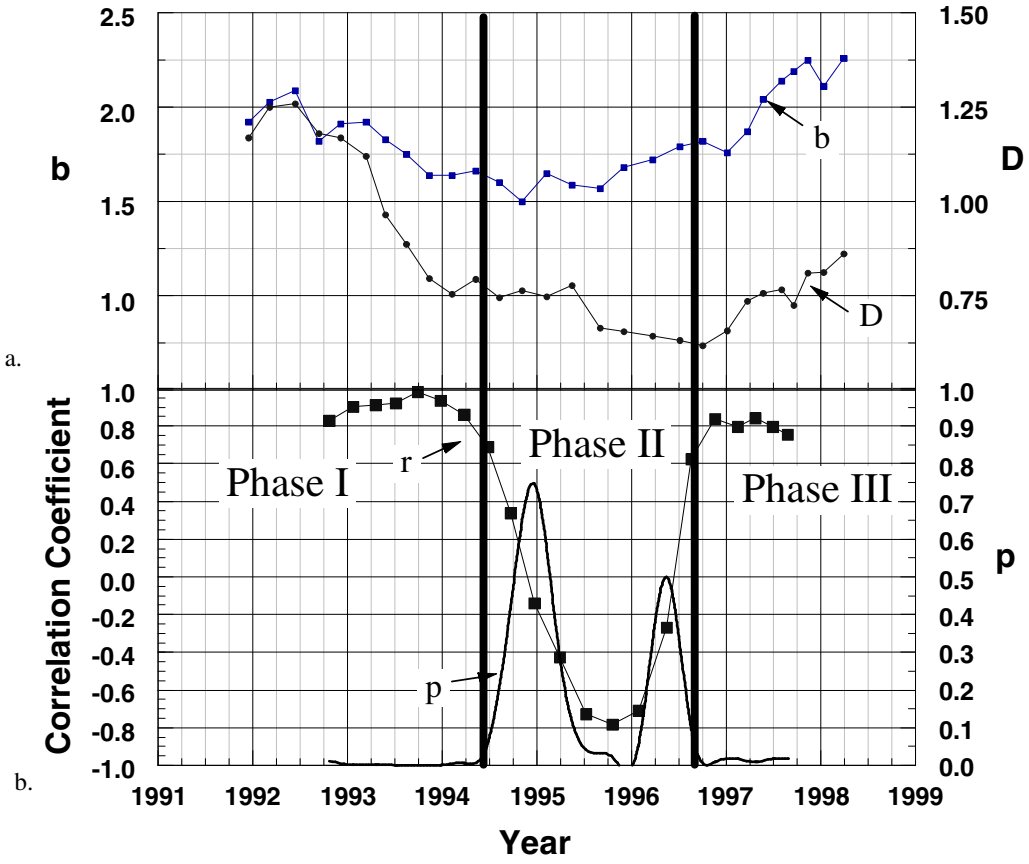
a.
b.
b
D
p
Correlation Coefficient
Year
Phase I
Phase II
Phase III
r
p
b
D
2.5
2.0
1.5
1.0
1.50
1.25
1.00
0.75
1.0
0.8
0.6
0.4
0.2
0.0
-0.2
-0.4
-0.6
-0.8
-1.0
0.9
0.7
0.5
0.3
0.1
1991
1992
1993
1994
1995
1996
1997
1998
1999

Figure 6

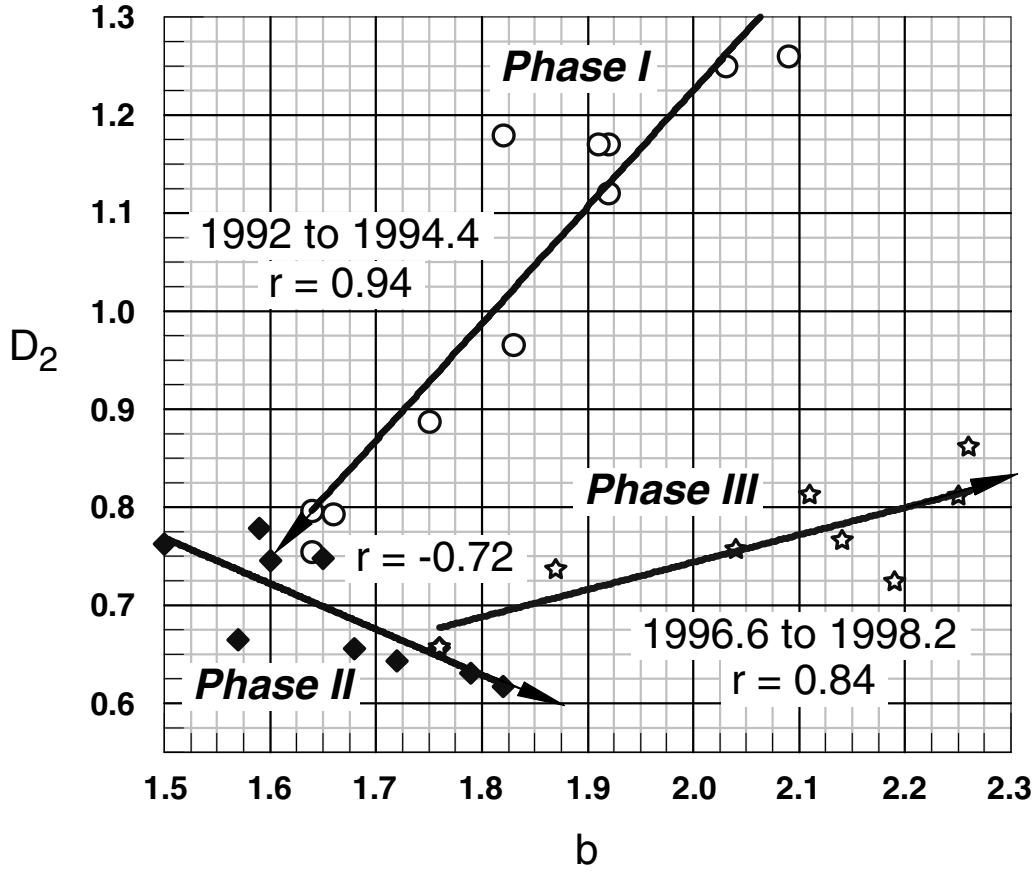
1.3
1.2
1.1
1.0
0.9
0.8
0.7
0.6
D2
Phase I
1992 to 1994.4
r = 0.94
Phase III
r = -0.72
1996.6 to 1998.2
r = 0.84
Phase II
1.5
1.6
1.7
1.8
1.9
2.0
2.1
2.2
2.3
b

Figure 7

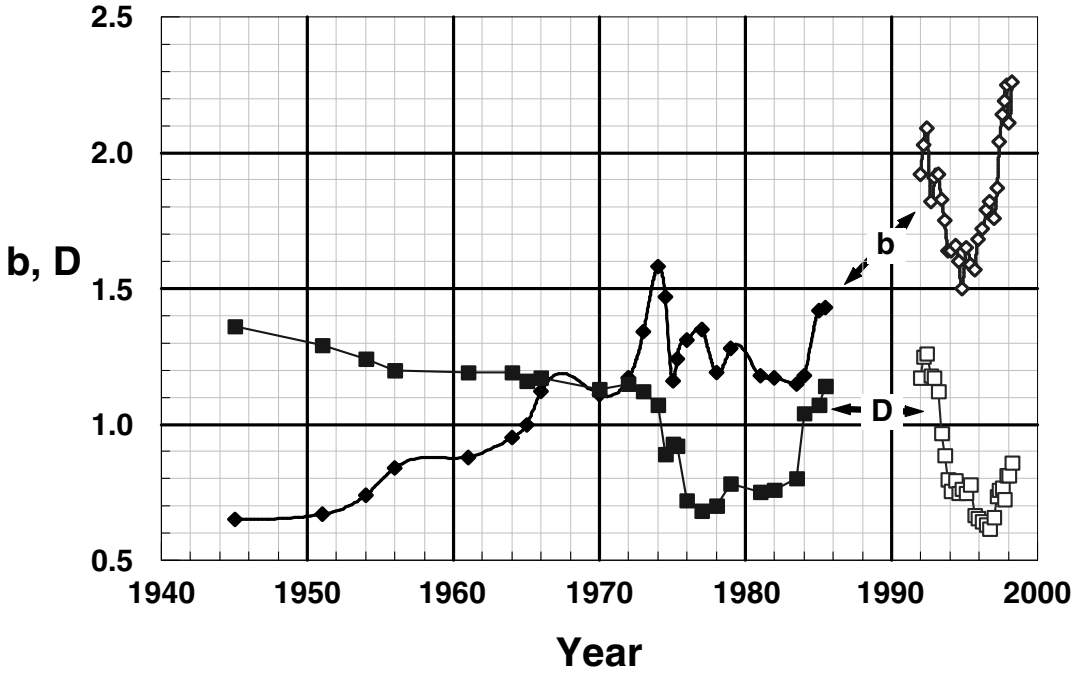

Figure 8